

A Monomeric Mn^{III}–Peroxo Complex Derived Directly from DioxygenRyan L. Shook,[†] William A. Gunderson,[‡] John Greaves,[†] Joseph W. Ziller,[†] Michael P. Hendrich,[‡] and A. S. Borovik^{*,†}

Department of Chemistry, University of California—Irvine, 1102 Natural Sciences II, Irvine, California 92697-2025, and Department of Chemistry, Carnegie Mellon University, Pittsburgh, Pennsylvania 15213

Received April 15, 2008; E-mail: aborovik@uci.edu

The binding and activation of dioxygen is an essential process in synthetic and biological chemistry.¹ The activation processes are often proposed to involve formation of peroxometal complexes, as exemplified by bleomycin and the mono-oxygenases cytochromes P450.² It is generally agreed that the initial steps in the O₂ binding/activation process in these enzymes involve a superoxoiron(III) intermediate that converts to a hydroperoxoiron(III) species through addition of an electron and proton. In this report, we demonstrate that a similar O₂ to peroxo conversion is operable in a synthetic manganese system.

The observation of synthetic monomeric peroxometal complexes is frequently difficult because of their inherent reactivity. This is especially true for peroxomanganese complexes, where the Mn^{IV}₂(μ-1,2-peroxo) complex of Wieghardt is the only O₂-derived system that has been structurally characterized.^{3,4} Others have found that treating Mn^{II} or Mn^{III} complexes with superoxides⁵ or peroxides⁶ produce systems with monomeric peroxomanganese centers—this approach has yielded a handful of complexes at low temperatures that were stable enough to be characterized. We have been investigating the interactions of dioxygen with manganese complexes containing intramolecular hydrogen bonding (H-bond) networks.⁷ Our systems utilize urea-based tripodal ligands that provide H-bond donors to coordinated O-atom species. The Mn^{II} complexes of these ligands bind and activate dioxygen producing monomeric oxomanganese complexes.^{7,8} We have developed a hybrid ligand (H₃bupa) that combines two urea arms with one carboxamidopyridyl moiety⁹—the Mn^{II} complex of this ligand binds O₂ to produce a detectable peroxomanganese(III) species.

Preparation of the precursor **1** is outlined in Figure 1.¹⁰ Treating H₃bupa with 3 equiv of KH in dimethylacetamide (DMA) followed by 1 equiv of Mn(OAc)₂ afforded K[**1**] and 2 equiv of KOAc.

The molecular structure of **1** determined by X-ray diffraction shows a five-coordinate Mn^{II} complex, having a distorted trigonal bipyramidal geometry.¹⁰ The trigonal plane is defined by the deprotonated urea and pyridyl nitrogen atoms of [H₂bupa]³⁻; the apical N1 atom and carbonyl oxygen O1 from the deprotonated carboxamide occupy the axial positions. The remaining portions of the urea groups form the scaffolding of a cavity, in which NH groups are positioned inward toward atom O1. However, the N6(N7)···O1 distances are greater than 3.2 Å, distances that are too long for intramolecular H-bonds.

A new green species (**2**) is formed in approximately 50% yield¹¹ when [Mn^{II}H₂bupa]⁻ reacts with O₂ at room temperature. In DMA, the reaction is relatively slow (~30 min), yet the formation of **2** can be completed in approximately 10 min when 0.5 equiv of diphenylhydrazine (DPH) is added to the reaction mixture (Figure 1). The yield of **2** also increases to nearly 80% when using DPH,

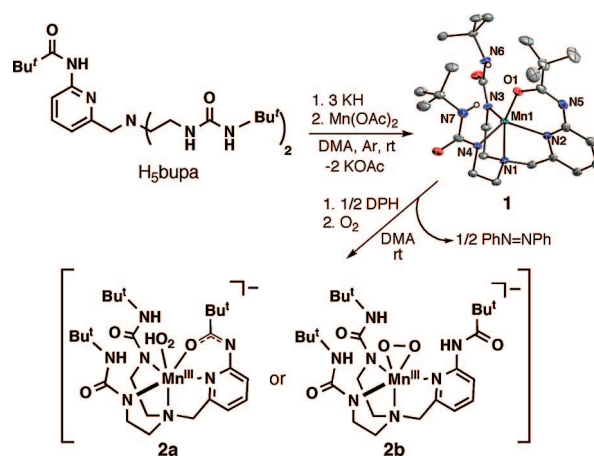


Figure 1. Preparative routes for **1** and **2**, showing two possible tautomers for **2**. The thermal ellipsoid plot of [Mn^{II}H₂bupa]⁻ is drawn at the 50% probability level, and non-urea hydrogen atoms are omitted for clarity. Selected distances (Å): Mn1–N1, 2.275(3); Mn1–N2, 2.214(3); Mn1–N3, 2.100(3); Mn1–N4, 2.125(3); Mn1–O1, 2.070(2).

which is converted to azobenzene (>95% yield). Monitoring the reactions with optical spectroscopy shows that **2** has a visible absorbance band at $\lambda_{\text{max}} \approx 660$ nm and a shoulder at 490 nm (Figure S1).¹² Similar spectra have been reported for Mn^{III} complexes containing a coordinated peroxo ligand.^{5d,6b}

The oxygenation of **1** was followed by electron paramagnetic resonance (EPR) spectroscopy (Figure S2). Perpendicular-mode X-band EPR spectra of [Mn^{II}H₂bupa]⁻ reveal the complex as a nearly axial $S = 5/2$ spin system with a large zero-field splitting constant of $D \sim 0.3$ cm⁻¹. After exposure to O₂, the $S = 5/2$ signal decreases as a new parallel-mode EPR signal associated with **2** appears at a g value of 8.2 (Figure 2A). A quantitative simulation of the signal (Figure 2B) indicates an $S = 2$ ground state with a six-line ($I = 5/2$) hyperfine splitting of $a = 57$ G. Variable temperature studies determined that the signal is from the ground doublet with $D = -2.0(5)$ cm⁻¹. The spin state, zero-field splitting, and hyperfine constant are in agreement with other known monomeric Mn^{III} species.^{5d,13} Moreover, the negative sign for the axial zero-field splitting constant is consistent with tetragonally elongated octahedral coordination geometry. The simulations also indicate that **2** accounts for 80(10)% of the Mn in the sample. In perpendicular-mode, this sample also showed the signal of the initial Mn(II) complex (6%) and a mixed valent species at $g = 2$ (4%). The parallel-mode signal vanishes after prolonged incubation (6 h) at room temperature—the identity of the resultant species are under investigation.

Isotopic labeling studies support the presence of a peroxo ligand coordinated to the Mn^{III} center in **2**. Solution FTIR spectra recorded at room temperature contained a peak at 885 cm⁻¹ for **2** prepared

[†] University of California—Irvine.[‡] Carnegie Mellon University.

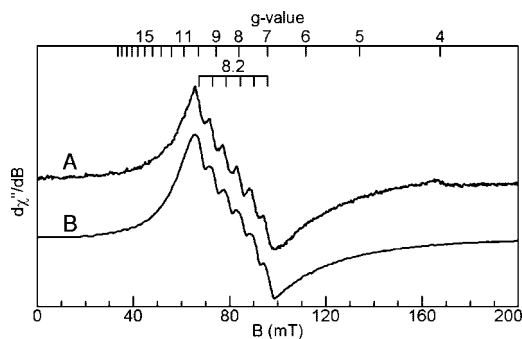


Figure 2. Parallel-mode EPR spectrum (A) and simulation (B) of **2** (10 mM in DMF) recorded at 11 K. Microwave frequency and power, 9.379 GHz, 0.2 mW; modulation, 10 G. Simulation parameters: $S = 2$, $g = 2.0$, $D = -2 \text{ cm}^{-1}$, $E/D = 0.13(3)$, $A = 160 \text{ MHz}$.

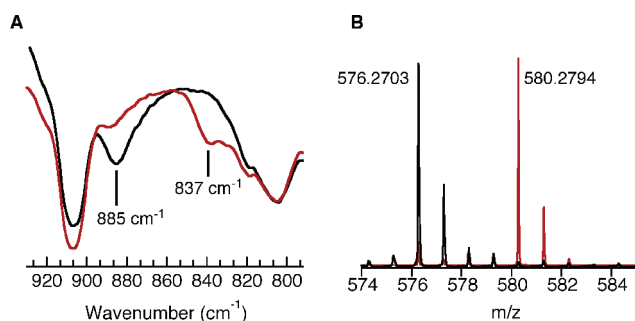
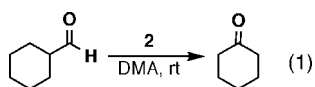


Figure 3. FTIR (A) and negative-mode ESI-MS (B) spectra of **2** after exposure to $^{16}\text{O}_2$ (black) and $^{18}\text{O}_2$ (red) collected from DMA solutions at room temperature.

under a $^{16}\text{O}_2$ atmosphere (Figure 3A). The ^{18}O -isotopomer can be prepared from $^{18}\text{O}_2$, causing a shift in the peak to 837 cm^{-1} . The observed vibrational change between the two isotopomers is as expected based on a harmonic O—O oscillator ($\nu(^{16}\text{O}_2)/\nu(^{18}\text{O}_2) = 1.06$; calcd = 1.07).¹⁴ These vibrational values are in the range normally observed for other metal-based peroxo systems. For instance, the η^2 -peroxoMn^{III}(Tp)¹⁵ complexes of Kitajima, formed using H_2O_2 , have FTIR-active peaks at 892 cm^{-1} that were assigned to $\nu(\text{O}_2)$.^{6a} The electrospray ionization mass spectrum (ESI-MS) of **2** prepared with $^{16}\text{O}_2$ exhibits a strong ion with a mass-to-charge ratio (m/z) of 576.2703 (Figure 3B), a shift of 33 mass units from the peak associated with **1** (Figure S3). The mass and calculated isotopic distribution corresponds to the addition of a hydroperoxo ligand to **1** (calcd, 576.2706; Figure S4A). Furthermore, when **2** was prepared from $^{18}\text{O}_2$, the molecular ion peak shifts by 4 mass units (Figure 3B) to a m/z of 580.2794 (calcd, 580.2792; Figure S4B).

Preliminary reactivity studies indicate that **2** leads to the oxidative deformylation of aldehydes. For instance, treating **2** with cyclohexanecarboxaldehyde afforded cyclohexanone as the only GC–MS detectable product in an unoptimized yield of 40% (eq 1). Note that deformylation reactions are known for iron(III)¹⁶ and manganese(III)^{6b} peroxo complexes.



The spectroscopic, mass spectrometry, and reactivity results are consistent with **2** being a monomeric peroxomanganese(III) complex. A possible mechanism for its formation would involve a superoxomanganese(III) intermediate that reacts with solvent or

external substrates, such as DPH, via a H-atom abstraction process to initially produce a η^1 -hydroperoxoMn(III) complex (Figure 1, **2a**). The reduction and protonation of the superoxo ligand mirrors steps proposed during turnover in cytochrome P450. The tautomeric η^2 -peroxomanganese(III) species (Figure 1, **2b**) could be formed from **2a** by intramolecular proton transfer from the hydroperoxo to the carboxamido component of the tripodal ligand. In this pathway, the pivaloylamide moiety is re-formed to provide an additional H-bond donor within the cavity. At present, we cannot distinguish between these two structural possibilities. Nevertheless, our findings establish that a mononuclear peroxoMn(III) can be produced from O_2 at room temperature.

Acknowledgment is made to the NIH (GM050781 to A.S.B.; GM77387 to M.P.H.) for financial support.

Supporting Information Available: Experimental details for all chemical reactions and figures for all spectra. This material is available free of charge via the Internet at <http://pubs.acs.org>.

References

- (1) Borovik, A. S.; Zart, M. K.; Zinn, P. J. In *Activation of Small Molecules: Organometallic and Bioinorganic Perspectives*, Tolman, W. B., Ed.; Wiley-VCH: Weinheim, Germany, 2006; pp 187–234, and references therein.
- (2) (a) *Cytochrome P450: Structure, Mechanism, and Biochemistry*, 3rd ed.; Ortiz de Montellano, P. R., Ed.; Kluwer Academic/Plenum Publishers: New York, 2005. (b) *Comprehensive Coordination Chemistry II*; Que, L., Jr., Tolman, W. B., Eds.; Elsevier: Oxford, 2004; Vol. 8. (c) Decker, A.; Chow, M. S.; Kemsley, J. N.; Lehnert, N.; Solomon, E. I. *J. Am. Chem. Soc.* **2006**, *128*, 4719–4733. (d) Groves, J. T.; Han, Y.-Z. In *Cytochrome P-450. Structure, Mechanism and Biochemistry*; Ortiz de Montellano R. R., Ed.; Plenum Press: New York, 1995; pp 3–48.
- (3) Bossek, U.; Weyhermüller, T.; Wieghardt, K.; Nuber, B.; Weiss, J. *J. Am. Chem. Soc.* **1990**, *112*, 6387–6388.
- (4) Dioxygen adducts of manganese porphyrins have been observed at low temperatures: (a) Weschler, C. J.; Hoffman, B. M.; Basolo, F. *J. Am. Chem. Soc.* **1975**, *97*, 5278–5280. (b) Hoffman, B. M.; Weschler, C. J.; Basolo, F. *J. Am. Chem. Soc.* **1976**, *98*, 5473–5482.
- (5) (a) Shirazi, A.; Goff, H. M. *J. Am. Chem. Soc.* **1982**, *104*, 6318–6322. (b) Groves, J. T.; Watanabe, Y.; McMurry, T. J. *J. Am. Chem. Soc.* **1983**, *105*, 4489–4490. (c) VanAtta, R. B.; Strouse, C. E.; Hanson, L. K.; Valentine, J. S. *J. Am. Chem. Soc.* **1987**, *109*, 1425–1434. (d) Groni, S.; Blain, G.; Guillot, R.; Polcar, C.; Anxolabehere-Mallart, E. *Inorg. Chem.* **2007**, *46*, 1951–1953.
- (6) (a) Kitajima, N.; Komatsuzaki, H.; Hikichi, S.; Osawa, M.; Moro-oka, Y. *J. Am. Chem. Soc.* **1994**, *116*, 11596–11597. (b) Seo, M. S.; Kim, J. Y.; Annaraj, J.; Kim, Y.; Lee, Y.-M.; Kim, S.-J.; Kim, J.; Nam, W. *Angew. Chem., Int. Ed.* **2007**, *46*, 377–380.
- (7) Borovik, A. S. *Acc. Chem. Res.* **2005**, *38*, 54–61, and references therein.
- (8) Parsell, T. H.; Behan, R. K.; Hendrich, M. P.; Green, M. T.; Borovik, A. S. *J. Am. Chem. Soc.* **2006**, *128*, 8728–8729.
- (9) (a) Wada, A.; Harata, M.; Hasegawa, K.; Jitsukawa, K.; Masuda, H.; Mukai, M.; Kitagawa, T.; Einaga, H. *Angew. Chem., Int. Ed.* **1998**, *37*, 798–799. (b) Marquie Rivas, J. C.; Salvagni, E.; Parsons, S. *Dalton Trans.* **2000**, 4185–4192. (c) Rudzka, K.; Arif, A. M.; Berreau, L. M. *J. Am. Chem. Soc.* **2007**, *129*, 17018–17023.
- (10) Full experimental details are found in Supporting Information.
- (11) Yields are obtained from EPR simulations using SpinCount developed by one of the authors (M.P.H.).
- (12) The extinction coefficient for this peak is less than $300 \text{ M}^{-1} \text{ cm}^{-1}$.
- (13) (a) Campbell, K. A.; Yikilmaz, E.; Grant, C. V.; Gregor, W.; Miller, A.-F.; Britt, R. D. *J. Am. Chem. Soc.* **1999**, *121*, 4714–4715. (b) Campbell, K. A.; Force, D. A.; Nixon, P. J.; Dole, F.; Diner, B. A.; Britt, R. D. *J. Am. Chem. Soc.* **2000**, *122*, 3754–3761. (c) Campbell, K. A.; Lashley, M. R.; Wyatt, J. K.; Nantz, M. H.; Britt, R. D. *J. Am. Chem. Soc.* **2001**, *123*, 5710–5719. (d) Krzystek, J.; Telser, J.; Hoffman, B. M.; Brunel, L.-C.; Licoccia, S. *J. Am. Chem. Soc.* **2001**, *123*, 7890–7897.
- (14) The difference of 48 cm^{-1} between the $\nu(\text{O}_2)$ of the two isotopomers is similar to those reported for $\text{Fe}^{\text{III}}\text{—OOH}$ and $\text{Fe}^{\text{III}}\text{—OO}$ complexes: Roelfes, G.; Vrajmasu, V.; Chen, K.; Ho, R. Y. N.; Rohed, J.-U.; Zondervan, C.; Crois, R. M.; Schudde, E. P.; Lutz, M.; Spek, A. L.; Hage, R.; Feringa, B. L.; Münck, E.; Que, L., Jr. *Inorg. Chem.* **2003**, *42*, 2639–2653.
- (15) Tp, hydrotris(3,5-*i*Pr-pyrazolyl)borate.
- (16) (a) Vaz, A. D. N.; Roberts, E. S.; Coon, M. J. *J. Am. Chem. Soc.* **1991**, *113*, 5887–5889. (b) Selke, M.; Sisemore, M. F.; Valentine, J. S. *J. Am. Chem. Soc.* **1996**, *118*, 2008–2012. (c) Wertz, D. L.; Sisemore, M. F.; Selke, M.; Driscoll, J.; Valentine, J. S. *J. Am. Chem. Soc.* **1998**, *120*, 5331–5332. (d) Goto, Y.; Wada, S.; Morishima, I.; Watanabe, Y. *J. Inorg. Biochem.* **1998**, *69*, 241–247.

JA802775E